Solar Cell Cooling and Heat Recovery in a Concentrated Photovoltaic System

Marco Cozzini*[1]
[1]Fondazione Bruno Kessler (FBK), Renewable Energies and Environmental Technologies (REET) Unit, Via Sommarive 18, 38123 Trento, Italy
*Corresponding author: cozzini@fbk.eu

Abstract: Concentrated photovoltaic systems are being widely investigated, aiming at improving the cost-efficiency balance in the solar energy field. An important issue is given by cell cooling, as the cell efficiency and stability typically decreases with temperature. On the other hand, the extracted heat can be recovered for cogeneration purposes (e.g., building heating), provided a suitable temperature is obtained. In order to find a viable compromise, it is crucial to introduce an efficient heat exchanger between the cell and the coolant fluid. In the present application, Comsol Multiphysics has been used to simulate the full 3D system provided by a solar cell coupled to a micro heat exchanger. The analysis includes both fluid dynamics (laminar regime) and heat transfer effects, also considering the thin insulating layers provided by the dielectric materials in the cell packaging. The resulting operating temperature and heat transfer performances of the system are calculated.

Keywords: Fluid dynamics, heat transfer, heat exchangers, concentrated photovoltaics.

1. Introduction

The renewable source provided by solar energy is expected to become one of the key ingredients of the future energy market. Several solar technologies are constantly being improved in order to obtain competitive prices with respect to traditional non-renewable resources.

A widely investigated solution is provided by concentrated photovoltaic (CPV) systems. CPV installations require a sun tracking system and suitable optics to concentrate the incoming radiation on a small area, where high-efficiency photovoltaic (PV) cells are typically located. The system can become more convenient than a conventional flat PV panel plant provided the costs of the additional components are balanced by a higher efficiency and/or by the savings deriving from the smaller amount of employed solar cells. The key point in favor of CPV versus PV systems is due to the fact that optical collectors (mirrors, lenses) have a lower cost per unit area than solar cells, though recent improvements in mass production of conventional silicon cells have reduced this margin. On the other hand, practical limits on the attainable concentration factors (which require demanding tracking performances at high values), optical losses, and the restriction to direct radiation for CPV systems (the amount of diffused radiation is not negligible in several climatic conditions) make the challenge quite difficult.

A possibly crucial ingredient to be included in the comparison between concentrating and non-concentrating photovoltaic systems is their suitability for the cogeneration of heat, obtaining PVT (PV thermal) or CPVT (CPV thermal) systems. Indeed, due to the limited efficiency of solar cells, the majority of the incoming radiation cannot be converted into electrical energy and is dissipated into heat. For CPV systems, where heat fluxes can approach values as high as 100 W/cm^2, cell cooling has to be explicitly taken into account in order to avoid excessive cell temperatures (see Ref. [1] for a review). Recovering this thermal energy for heating purposes would provide an added value to the plant. Several issues are related to the practical exploitability of the available heat: a key point for the determination of possible destinations (e.g., industrial processes or building heating) of this resource is anyway given by the cell operating temperature.

Solar cells perform better at lower temperatures. As the most valuable outcome of solar panels is electricity, this poses important constraints when considering cogeneration of heat. However, the temperature coefficient (yielding the temperature dependence of the cell efficiency) and the maximum operating temperature can vary significantly with the cell type. For example, triple junction cells, besides reaching almost twice the efficiency of silicon cells, can operate at temperatures about 20 – 30

K higher. On the other hand, triple junction cells are more expensive and are better exploited at high concentration levels.

In the MiSTICo (Micro Sistemi e Tecnologie Innovative per Cogenerazione da energia solare) project, featuring a collaboration between several units of the Bruno Kessler Foundation (Trento, Italy) and the Mechanical Department of the Bologna University (Italy), a prototype of a CPVT system is being realized. As the economic viability of CPV/CPVT systems depends on the numerous factors discussed above, the project includes the investigation of the system efficiency with different types of cells and concentration levels. The heat cogeneration is based on the active cooling of solar cells through a closed circuit filled with purified water. A fundamental ingredient in this system is provided by the heat exchanger located in contact with the cell packaging. Such component must minimize the temperature gap between the cell and the vector fluid, in order to allow for the highest possible electrical efficiency at the chosen coolant working temperature. The present work describes the design and simulation with Comsol Multiphysics of a micro-channel heat exchanger suitable for mono-crystalline Si-cells at 160 suns, the first kind of cells to be tested in the project. The applicability of the same heat exchanger to high concentration triple junction cells will be also discussed.

2. CPVT system and cooling circuit

Heat is transferred from the cell to the vector fluid through a heat exchanger designed to be mounted on the back of the cell packaging. Two kind of cells are being considered in the project: triple junction cells for high concentration levels, reaching efficiencies of the order of 35 - 40 % at about 1000 suns, and medium concentration mono-crystalline silicon cells, with efficiencies of the order of 20 % at about 100 suns. In both cases the size of the cell is assumed to be 1 cm × 1 cm. While the higher efficiency of triple junction cells seems extremely promising, the demanding requirements imposed by high concentration levels in terms of sun tracking precision make the convenience of one system with respect to the other still uncertain.

In both cases, an important issue is given by cell cooling, as the cell efficiency and stability typically decreases with temperature (especially in the case of silicon). At a concentration factor of 1000 suns an energy flux of about 100 W/cm^2 is present, the 60 % of which is expected to be transferred to the fluid as heat flux, requiring quite efficient cooling methods in order to keep the cell temperature at reasonable values.

The reported analysis includes fluid dynamics (laminar regime) and heat transfer effects in both the micro-channel heat exchanger and the cell packaging, as the thin electrically insulating layer present in the latter significantly affects the system heat conduction.

1.1 Cell Packaging

Cell packaging plays an important role from the point of view of heat transfer and the corresponding thermal resistance has to be carefully taken into account. In the packaging solution adopted for the considered Si-cells, the cell is soldered to an insulated metal substrate (IMS) containing the printed circuit for the cell connections. This is basically a printed circuit board (PCB) where the usual support material (e.g., FR4) is replaced by aluminum, covered by an insulating layer with relatively high thermal conductivity (see below). Other solutions more suitable to triple junction cells will be explored in the next project activities..

The IMS composition is as follows: 70 μm of copper layer (thermal conductivity of about 400 W/(m·K)), 100 μm of dielectric layer (thermal conductivity 1.8 ÷ 3 W/(m·K)), and 1.5 mm of aluminum base (thermal conductivity 222 W/(m·K)). Before soldering the cell on the copper layer, the deposition of an additional gold layer is required. The small thickness of such layer (< 4 μm) makes it negligible for thermal calculations.

1.2 Heat exchanger design

For the first prototype of the heat exchanger a simple design with parallel micro-channels has been chosen. There is a rich literature about micro-channel heat exchangers, mainly applied as heat sinks for high-power electronics (see, e.g., Ref. [2] and references therein). Configurations with various levels of complexity have been tested [3 – 5], promoting the heat transfer coefficient with the enhanced fluid/solid interfaces obtained with dense arrays of small channels. On the other hand, small hydraulic diameters can give rise to high pressure drops, an undesired feature in solar applications where the resulting pumping power affects the overall system efficiency.

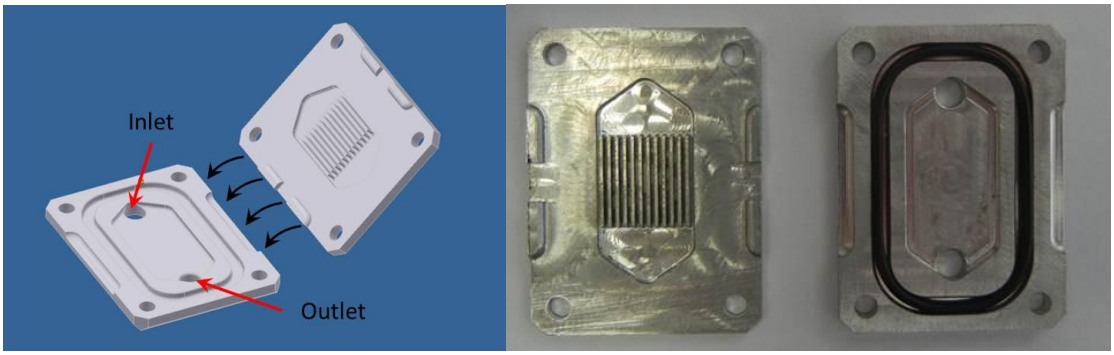

Figure 1. Geometry of the prototypal heat exchanger (left image: CAD drawings; right image: prototype to be tested). Apart from the mechanical details related to mounting (screw holes, matching pins, seal seat), one can recognize the inlet and outlet holes in the bottom part and the fins corresponding to micro-channel walls in the upper part.

In the present design (see Figure 1), a compromise has been adopted for the micro-channel size, taking into account head losses and manufacturing simplicity. For the considered application, it is indeed important to develop a cost competitive solution. The size of the channels has hence been kept within the limits achievable with standard machining tools. Each channel is 12.5 mm long and has a rectangular cross section with a width of 0.5 mm and a height of 2 mm. An aluminum prototype has already been realized by milling, splitting the exchanger in a top (where the channel walls were milled as thin fins) and a bottom component. The two components perfectly match together so that the bottom component covers the fins giving rise to 13 micro-channels. Once assembled, the exchanger has a thickness of 5 mm, with a basis given by a 3 cm × 4 cm rectangle.

It is crucial to ensure a good contact between the cell packaging and the heat exchanger, and between the exchanger pieces as well. To this purpose, a layer of highly conductive thermal grease (thermal conductivity 10.5 W/(m·K)) has to be smeared on the aluminum surfaces before mounting and the components are fixed together with suitable screws (ensuring also a proper compression of the sealing ring). The thickness of each grease layer has been assumed to be 0.1 mm in the simulations.

3. Use of COMSOL Multiphysics

The numerical simulations have been performed with Comsol Multiphysics 4.2a. The Heat Transfer Module was employed, with the Conjugate Heat Transfer physics interface. Fluid dynamics was solved within the laminar regime (Navier-Stokes equations). As water properties do not change significantly in the considered temperature range (water inlet temperature of 40 °C), an unidirectional coupling with the heat transfer equation has been used.

Two groups of simulations are reported in the following. First, the overall micro heat exchanger was studied. By exploiting the system symmetry, calculations were performed on the reduced geometry corresponding to one half of the exchanger (see Figure 2). Second, a detailed analysis of a single channel was carried out. Here, the situation corresponding to the case of an infinite array of parallel channels was reproduced by using symmetric boundary conditions (see Figure 3). The resulting behavior is expected to be roughly similar to that of the central channels of the exchanger, where the effects of the array border are relatively weak. The reduced geometry of a single channel was used to perform convergence studies, thereby checking result accuracy.

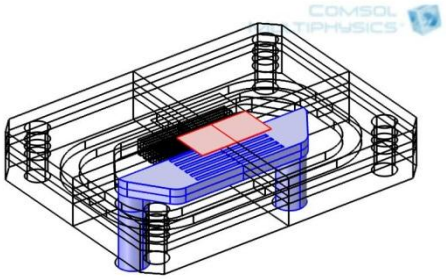

Figure 2. Exchanger geometry in Comsol. Only half of the geometry has to be simulated, thanks to symmetry. Blue: simulated fluid domain. Red: simulated heat flux area (cell). The same symmetry was applied to the simulated solid domain.

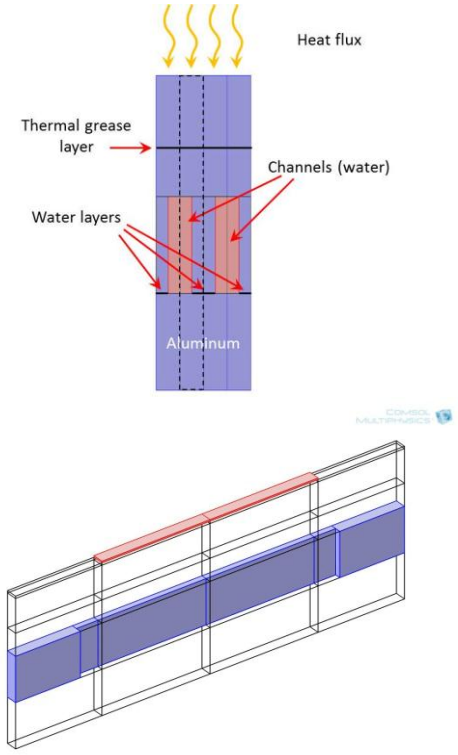

Figure 3. Reduced geometry for the single channel simulations. The upper panel shows a cross section with two parallel channels, where the dashed area corresponds to the reduced geometry (lower panel).

3.1 Boundary conditions

For the fluid dynamic problem, a velocity profile corresponding to a global flow rate of 5 ml/s was imposed at the inlet, while a constant pressure was imposed at the outlet. No-slip boundary conditions were assumed at the walls. Symmetry was exploited with usual symmetric boundary conditions where necessary.

For the thermal problem, a constant irradiation flux was assumed on the boundary corresponding to the solar cell. The chosen power was matched to the concentration level, decreased by the amount converted into electrical energy. A constant fluid temperature of 40 °C was assumed for the incoming fluid, purely convective outflow was imposed at the outlet. All the remaining boundaries were insulated, neglecting other thermal losses (which are indeed expected to be quite small in the prototype, where a teflon casing has been realized for the heat exchanger).

3.2 Mesh and solver settings

For the full exchanger an unstructured mesh with tetrahedral elements was used. The mesh was refined within the micro-channels in order to ensure at least 6 elements in the transverse direction.

For the case of the single channel a combination of mapped and swept meshes was used, allowing for a careful control of the number of elements in any direction.

The PARDISO solver was used. Typically, the fluid dynamic problem was first solved independently, for easier convergence, then the temperature variable was included.

4. Results

In this section we discuss the results for both geometries under the operating conditions expected for Si-cells at 160 suns. Considering a cell electrical efficiency of 20 %, we assumed a heat flux of 12.8 W/cm^2. Water inlet temperature was fixed at 40 °C.

Micro heat exchanger analysis. A flow rate of 5 ml/s was applied to the exchanger. A parabolic velocity profile was applied at the inlet, which is given by a circular channel with a diameter of 4 mm. Some attention was devoted in the design to the flow distribution within the channels, in order to ensure a balanced flow rate in the different branches. See the upper panel of Figure 4 for the resulting velocity profile.

The pressure drop of the entire exchanger turns out to be less than 7 mbar at the considered flow rate. With the above heat flux, the temperature difference across the sole heat exchanger is found to be about 4 K; other 2 K of difference occur across the aluminum support of the packaging. The remaining layers of the packaging were not simulated here. Some slices of the temperature profile are shown in the lower panel of Figure 4.

The temperature distribution in the area corresponding to the cell position is not perfectly symmetric with respect to the cell center, showing the influence of the flow direction. The temperature profile of the cell is actually more uniform when including the dielectric layer (see later). As the cell efficiency is sensitive to the cell maximum temperature, uniform cell temperature profiles are desirable.

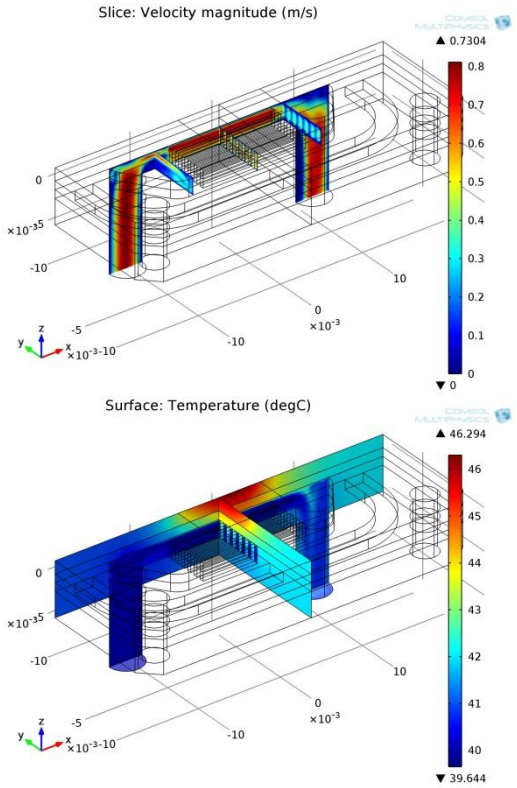

Figure 4. Velocity (upper panel) and temperature (lower panel) profiles within the heat exchanger. Flows enter at 40 °C from the bottom left circular channel. Heat flux: 12.8 W/cm^2 (Si-cell at 160 suns). The dielectric layer of the cell packaging is not included.

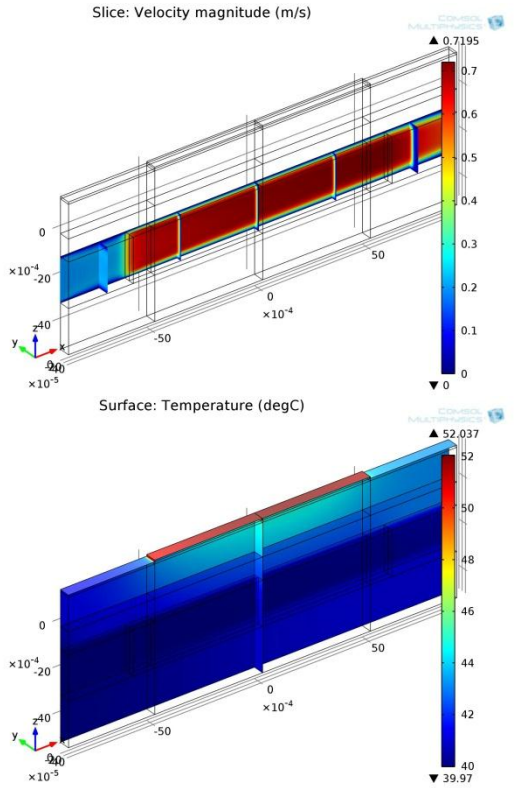

Figure 5. Velocity (upper panel) and temperature (lower panel) profiles within the single channel geometry. Flows enter at 40 °C from the left (constant velocity profile). Heat flux: 12.8 W/cm^2 (Si-cell at 160 suns). The dielectric and the copper layer of the cell packaging are visible in the plots.

Single channel analysis. The reduced geometry considered here corresponds to half of a single channel under periodic (symmetric) boundary conditions in the transverse direction. The flow rate was assumed to be equal to the average flow rate in the exchanger channels (i.e., half of 1/13 of 5 ml/s). Short inlet/outlet regions before the channel were included, in order to better compare with the heat exchanger geometry. In Figure 3 the fluid domain is highlighted in blue and the inlet/outlet regions (no lateral walls, vertical confinement only) correspond to the larger sections. The dielectric layer and copper (highlighted in red) layers of the packaging are also visible.

The single channel results are in general agreement with those for the exchanger. The possibility of computing the solution with quite accurate meshes (e.g., 20 elements across half of the channel width) allows here to get smoother profiles for the velocity field (Figure 5).

As far as the temperature is concerned, results are of the same order of those for the full system (4 K temperature difference across the exchanger, 2 K across the aluminum IMS base; see Figure 5). By explicitly simulating the dielectric layer and the copper layer where the cell is soldered, other 6 K of temperature difference were found (in the worst case scenario where the dielectric layer is assumed to have the lowest thermal conductivity in the interval declared by the supplier, i.e., 1.8 W/(m·K)).

The pressure drop across the channel structure was found to be of the order of 3 mbar, in agreement with the results on the exchanger geometry. The scaling of the pressure drop with the flow rate was also investigated, finding roughly a linear behavior, as expected in the laminar regime (for the exchanger flow rate of 5 ml/s, the Reynolds number Re is about 310 within the channel and about 1600 at the exchanger inlet).

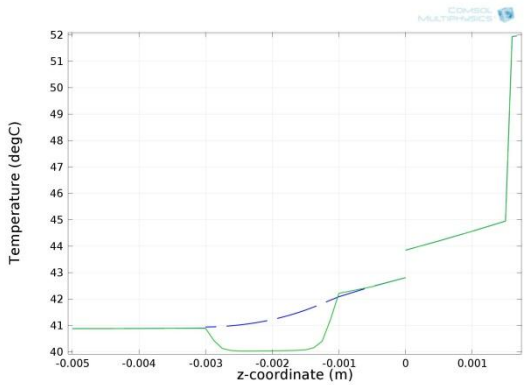

Figure 6. Temperature profiles in the vertical directions at half of the channel length. Green solid line: temperature along the line passing by the channel center. Blue dashed line: temperature along the line passing by the wall center.

In Figure 6 the temperature distribution in the vertical direction at half of the channel length is reported (see figure caption for more details). The great thermal resistance provided by the dielectric layer is evident. It is also possible to recognize the discontinuity arising from the inclusion of the thermal grease as a thin insulating layers.

5. Conclusions and perspectives

In this work, Comsol Multiphysics has been applied to the analysis of a micro heat exchanger at the moderate powers corresponding to Si-cells at 160 suns. Results showed a temperature difference of about 10 K between the cell temperature and the inlet cooling fluid temperature, where the main contribution to the thermal resistance comes from the thin insulating layer present in the IMS packaging. The heat exchanger is therefore expected to exhibit satisfactory thermal performances in this regime. Moreover, with the relatively large channel size adopted here, low pressure drops are obtained. Experimental tests will be conducted on the prototype in a near future.

On the other hand, a natural question arises about how would such exchanger behave in the case of the higher heat fluxes given by triple junction cells. Simulations not reported here but analogous to those discussed in the text have shown that the present geometry is not very successful in the high concentration case, the main obstacle being provided by IMS layers. Future work will therefore include the identification of a more suitable packaging solution and/or the testing of different exchanger geometries. For example, some preliminary calculations involving impinging jets have yielded promising results. A proper implementation of this kind of flow could indeed allow a more direct access to the substrate, reducing contact problems among components and avoiding the need for expensive micromachining. See Ref. [6] for an optimized impinging jet application exploiting Comsol Multiphysics.

6. References

1. A. Royne *et al.*, Cooling of photovoltaic cells under concentrated illumination: a critical review, *Sol.Energy Mater. Sol. Cells*, **86**, 451 (2005)
2. M. G. Khan and A. Fartaj, A review on microchannel heat exchangers and potential applications, *Int. J. Energy Res.*, **35**, 553–582 (2011)
3. D. B. Tuckermann and R. F. W. Pease, High-performance heat sinking for VLSI, *IEEE Electron Device Lett.*, **2**, 126 (1981)
4. D. Copeland, Manifold microchannel heat sinks: Analysis and optimization, *Thermal Sci. Eng.*, **3**, 7 (1995)
5. Y. Wang and G.-F. Ding, Numerical analysis of heat transfer in a manifold microchannel heat sink with high efficient copper heat spreader, *Microsyst. Technol.*, **14**, 389 (2008)
6. E. M. Dede, Experimental Investigation of the Thermal Performance of a Manifold Hierarchical Microchannel Cold Plate, *InterPACK 2011 ASME Conf. Proc.*, **2**, 59 (2011)

7. Acknowledgements

The MiSTICo project is partially funded by Fondazione CARITRO (Trento, Italy).